

ORIGINAL RESEARCH ARTICLE

Development of topical curcumin nanoemulsion and comparing its anticancer effects with oral curcumin in a syngeneic mouse model of breast cancer

Anupa Sivakumar^{1*}, **Sunil Pazhayannur Venkateswaran²**, **Htar Htar Aung¹**, **Jeya Seela Anandha Rao²**, **Ammu Kutty Radhakrishnan³**, and **Shadab Md⁴**

¹Department of Human Biology, School of Medicine, International Medical University, Kuala Lumpur, Malaysia

²Department of Pathology and Pharmacology, School of Medicine, International Medical University, Kuala Lumpur, Malaysia

³Food as Medicine Research Strength, Jeffrey Cheah School of Medicine and Health Sciences, Monash University Malaysia, Selangor, Malaysia

⁴Department of Pharmaceutics, Faculty of Pharmacy, King Abdulaziz University, Jeddah, Saudi Arabia

***Corresponding author:**

Anupa Sivakumar
(anupa_sivakumar@imu.edu.my)

Citation: Sivakumar A, Venkateswaran SP, Aung HH, Rao JSA, Radhakrishnan AK, Md S. Development of topical curcumin nanoemulsion and comparing its anticancer effects with oral curcumin in a syngeneic mouse model of breast cancer. *Cancer Plus*. 2025;7(1):96-108. doi: 10.36922/cp.8102

Received: December 20, 2024

1st revised: March 2, 2025

2nd revised: March 11, 2025

Accepted: March 21, 2025

Published online: April 15, 2025

Copyright: © 2025 Author(s). This is an Open-Access article distributed under the terms of the Creative Commons Attribution License, permitting distribution, and reproduction in any medium, provided the original work is properly cited.

Publisher's Note: AccScience Publishing remains neutral with regard to jurisdictional claims in published maps and institutional affiliations.

Abstract

Current breast cancer (BC) treatments often cause side effects, and prolonged use can lead to drug resistance. Hence, there is a demand for alternative treatment options for BC, particularly those utilizing natural compounds with better selectivity and lower toxicity. Curcumin (Cur) is a natural compound with anticancer effects but suffers from low bioavailability, accentuating the need for improved delivery systems. Transdermal drug delivery offers better patient compliance and site-specific delivery for improved treatment. In this study, a formulation of Cur-nanoemulsion (Cur-NE) was developed and characterized. The anticancer potential of the Cur-NE was evaluated using a syngeneic BC mouse model. Cancer was induced by injecting 4T1 murine mammary cancer cells into the breast pad of female Bagg Albino/c (BALB/c) mice. Treatments were started when the tumor was palpable on day 11. Tumor growth was monitored regularly. Upon sacrifice, the tumor, lungs, and liver were harvested from all animals for histopathological, immunohistochemistry (IHC), and gene expression analysis. Histological assessment revealed a higher percentage of necrosis area (25 – 70%) in tumor tissues from mice fed with Cur compared to animals fed with vehicle (10 – 50%) and those that received topical application of the Cur-NE (10 – 40%). The IHC analysis of the BC for biomarkers such as CD9, tissue inhibitor of metalloproteinases-1, and matrix metalloproteinase-13 showed higher immunoreactivity scores in the animals that received topical application of Cur-NE compared to the vehicle-fed group. The expression of four candidate genes (*CDH1*, *TWIST1*, apoptosis inhibitor-5, and *CD274*) was downregulated ($p < 0.05$) in the Cur-NE group compared to the group fed with Cur. These results suggest that topical application of Cur-NE had higher anticancer effects than oral administration of Cur, making it a promising approach for the treatment of BC.

Keywords: Curcumin; Nanoemulsion; Transdermal delivery; Breast cancer; Gene expression; Immunohistochemistry

1. Introduction

Breast cancer (BC) is the most common cancer in women worldwide and a leading cause of cancer-related mortality in women.¹ According to the GLOBOCAN 2022 cancer database, 2.2 million new cases of BC were reported globally, with 666,103 deaths. BC is the fourth most common cancer in women.² In Malaysia, the 2017 – 2021 National Cancer Registry report indicated that BC accounted for 19% of cancers in women, followed by colorectal cancers (13.5%).³ Although BC remains the fifth most common cause of death in women, survival rates have improved in recent years.⁴ For instance, early detection of BC is made possible through mammography, ultrasound, breast magnetic resonance imaging, and tissue biopsy.⁵ Furthermore, there are numerous options for the treatment and management of BC, which include combinations of surgery,⁶ radiation therapy,⁷ chemotherapy,⁸ hormonal therapy,⁹ and targeted therapy.¹⁰

Chemoprevention and treatment strategies are actively being explored to enhance bioavailability and efficacy while reducing the cost of care for cancer patients. Several Food and Drug Administration-approved drugs and monoclonal antibodies have been successfully used to treat BC. However, many of these drugs are associated with side effects that impact patients' quality of life, including low blood counts, hair loss, arthralgia and myalgia, peripheral neuropathy,¹¹ cognitive dysfunction,¹² nausea and vomiting,¹³ diarrhea,¹⁴ endometrial carcinoma,¹⁵ thromboembolic disorders,¹⁶ and drug resistance with long-term therapy.¹⁷

Recent research explored novel therapeutics for complex diseases. Natural compounds have been used throughout medical history to treat cancers due to their efficacy through unique mechanisms, low toxicity, safety, and general availability.¹⁸ One such compound, curcumin (Cur), a naturally occurring polyphenolic compound extracted from *Curcuma longa* Linn, exhibits strong anti-inflammatory properties.¹⁹ Its anti-inflammatory effects are attributed to its ability to inhibit (i) arachidonic acid metabolism, (ii) the cyclooxygenase pathway, (iii) the lipoxygenase pathway, (iv) the pro-inflammatory cytokine production, and (v) nuclear factor kappa B activation.¹⁸ Cur, classified as a "generally recognized as safe" substance, is characterized by stable metabolism and low toxicity, making it a promising candidate for medicinal development.²⁰ However, its poor water solubility at acidic or neutral pH, extensive degradation in alkaline environments, and rapid first-pass metabolism into inactive metabolites significantly limit its systemic bioavailability.^{21,22} Therefore, several approaches have been investigated to increase Cur biological efficacy, including its chemical derivatization,

complex formation, macromolecular interactions, and nanoscale drug delivery systems.²³

Among these strategies, nanoemulsions (NE) have emerged as a promising technology for improving drug solubility, stability, and bioavailability across various therapeutic applications.²⁴ Their ability to bypass first-pass metabolism and minimize long-term side effects makes them valuable for optimizing drug delivery and enhancing patient outcomes.^{25,26}

BC continues to be a predominant cause of cancer-related mortality globally, with existing treatment modalities frequently constrained by adverse effects and resistance mechanisms.²⁷ In light of these challenges, there is an increasing interest in adjunctive therapeutic techniques that can improve treatment efficacy while reducing toxicity. Cur, a polyphenolic substance from *Curcuma longa*, exhibits notable anticancer capabilities, encompassing anti-inflammatory, pro-apoptotic, and anti-metastatic actions.²⁸ Nonetheless, its clinical application is impeded by inadequate aqueous solubility, fast metabolism, and diminished systemic bioavailability. Nanoemulsification has emerged as a promising drug delivery method to address these constraints, improving Cur solubility, stability, and bioavailability. The development of Cur-NE may offer a more efficacious method to harness its therapeutic potential in BC treatment.²³ Hence, the main objective of this study was to develop a stable Cur-NE formulation, characterize its physiochemical properties, and evaluate its anticancer effects through transdermal delivery in a syngeneic BC mouse model. In addition, gene expression analyses were conducted to elucidate potential underlying mechanisms.

2. Materials and methods

This study was conducted in two phases: (i) development and characterization of Cur-NE formulation and (ii) evaluations of its anticancer potential in a syngeneic mouse model of BC.

2.1. Test compounds, chemicals, and consumables

Cur, purchased from Sisco Research Laboratories (India), possessed a purity of 95% and the preparation passed the IR spectrum test. All chemicals and reagents used for this research were of analytical grade. Propylene glycol monocaprylate (Capryol 90) was purchased from Gattefosse Pharma (Malaysia). Polyoxyethylene sorbitan monolaurate (Tween-20) was purchased from Sigma-Aldrich (Malaysia). Different surfactants and cosurfactants (Cremophore EL, Labrafill M1944CS) were obtained from Sigma-Aldrich. RPMI 1,640 medium, fetal bovine serum (FBS), penicillin-streptomycin (10,000 U/mL), TrypLE™ Express reagent,

phenol red, phosphate-buffered saline (PBS, pH: 7.4), and RNase- and DNase-free ultrapure distilled water were purchased from GIBCO (USA). Dimethyl-54-sulfoxide was obtained from Sigma-Aldrich while (2-(4-iodophenyl)-3-(4-nitrophenyl)-5-(2,4-disulfophenyl)-2H-tetrazolium (WST-1) was from Roche Diagnostic GmbH (Germany). The oral gavage needle was purchased from Interfocus (England) while other syringes (1 mL, 10 mL, and 1 mL with a 27G needle) were from Terumo® (Japan). Digital caliper was obtained from eBioscience (USA).

2.2. Cell line

The 4T1 murine mammary cancer cells are adherent and cultured as the ATCC recommended. These cancer cells were isolated from BC in BALB/c mice.³⁶ Tumour growth induced in female syngeneic BALB/c mice resembles human stage IV BC regarding tumour growth and spread.³⁷

2.3. Mice models

Female BALB/c mice (6 weeks old) were purchased from an accredited local supplier (Chennur, Malaysia) and housed at the animal holding facility, International Medical University (IMU). The animals were acclimated for at least 5 days before starting the experiments. The experimental animals were housed in ventilated cages. The bedding for the cages and standard food pellets for the mice were from Chennur. The experimental animals had *ad libitum* access to water and food pellets throughout the study.

2.4. Selection of oil, surfactant, and co-surfactant for NE formulations

NE formulations containing Cur were prepared using a previously described method with slight modifications.³⁰ The first step was to screen excipients – such as oil, surfactant, and co-surfactant – to identify those providing maximum Cur solubility. Oils (Capryol 90, olive oil, soybean oil, corn oil, or sunflower oil), surfactants (Tween-20, Tween-80, Transcutol HP, Labrafil 2125), and the co-surfactant (ethanol) were evaluated individually. Each preparation was vortexed using a vortex mixer (fine polymerase chain reaction [PCR], Korea) for 20 min. The mixture was solubilized in a shaking incubator at 37°C for 72 h, periodically checked, and additional Cur was added if the solution became transparent. Thereafter, the samples were centrifuged (5,000 rpm, 20 min) and the supernatant was diluted with methanol. The samples were then quantified using an ultraviolet (UV)-spectrophotometer (Perkin Elmer, USA) at a wavelength of 421 nm that detects Cur. Excipients (oil, surfactant, and co-surfactant) that showed the highest solubility for Cur were selected for NE formulations.

2.5. Formulation of placebo and Cur-NE

A total of 5 mg of Cur was first dissolved in the oil phase, followed by the addition of a mixture of surfactant and co-surfactant (Smix). The mixture was vortexed for 15 min and subsequently subjected to ultra-sonification for another 15 min. Then, the aqueous phase was gradually added with continuous vortexing for 15 min to facilitate emulsification and ensure uniformity of the formulation. A placebo NE was prepared using the same method without Cur.

2.6. Thermodynamic stability tests

Drug-loaded NEs were subjected to thermodynamic stability testing, including centrifugation, heating-cooling cycles, and freeze-thaw cycles, to identify stable formulations. The selected stable formulations were centrifuged (5,000 rpm, 30 min) and observed for signs of cracking, creaming, or phase separation.³¹ Then, a heating-cooling cycle was performed, where the NEs were stored at alternating temperatures of 4°C and 40°C for 72 h at each temperature. Freeze-thaw stability was evaluated over three cycles, where formulations were alternately stored at –20°C and 25°C for 72 h per cycle.

2.7. Characterization and *in vitro* evaluation of Cur-NE formulation

2.7.1. Droplet size, polydispersity index (PDI), and zeta potential (ZP) analysis

The optimized Cur-NE formulation was diluted 100-fold and tested for droplet size, PDI, and ZP. The parameters were assessed using a Zetasizer (Nano ZSP, Malvern, UK).

2.7.2. pH and viscosity measurements

The pH was measured using a pH meter (FiveEasy pH meter F20, Mettler Toledo, Switzerland). The Cur-NE formulation was placed in a beaker and the pH was measured in triplicates at 25 ± 1°C. The viscosity of the formulation was determined using a cone and plate viscometer (RST Rheometer, Brookfield Ametek, USA) with spindle 50.2 at 10 rpm and 25°C ± 0.5°C.

2.7.3. Entrapment efficiency (EE) assessment

Cur EE in Cur-NE was determined by measuring the final Cur concentration after preparation and centrifugation. EE (%) was calculated using the following equation³²: (Actual drug loading)/(Theoretical drug loading) × 100; where actual drug loading (mg/g) is the measured amount of Cur in Cur-NE formulation and theoretical drug loading (mg/g) is the total amount of Cur used in formulation preparation.

2.8. Storage shelf life of Cur-NE formulation

The Cur-NE was stored for 60 days, and changes in Cur content and particle size of the droplets were monitored using the UV spectrophotometer and Zetasizer to assess stability over time.³³

2.9. *In vitro* release studies

In vitro release studies of the Cur-NE and Cur solutions were done using the Franz cell diffusion method, employing a synthetic membrane (Strat-M) in place of animal skin.³⁴ The membrane was clamped between the donor and receptor chambers of the Franz diffusion cell (Strat-M[®] Membrane, Merck Millipore Ltd., Ireland), with the shiny part of the membrane facing the donor chamber. Then, 1 mL of the sample was administered on the shiny surface of the membrane. The receptor compartment was filled with phosphate buffer (pH 7.4) and maintained at a constant temperature of $37 \pm 0.5^\circ\text{C}$ using a circulating water jacket and constant magnetic stirring (300 rpm). An aliquot (1 mL) of the sample was periodically (0, 1, 2, 3, 4, 5, 6, 7, and 8 h) drawn from the receptor compartment and replaced with an equal volume of fresh buffer. Cur concentration was quantified using a UV spectrophotometer at a wavelength of 421 nm.

2.10. *In vivo* studies

The experimental design for the development of the syngeneic BC mouse model is outlined in Figure 1.

2.10.1. Culture of murine mammary cancer cells

The 4T1 cells were cultured at 37°C in a humidified 5% CO_2 incubator and maintained in a complete medium consisting of RPMI 1640 medium, 10% FBS, 1% penicillin and streptomycin solution, 1% sodium pyruvate and 1%

HEPES.³⁵ When 4T1 cells reached 70% confluent, they were subcultured. Once the spent culture media was removed, the adherent cells were washed twice with sterile PBS. Then, 3 mL of TrypLE[™] Express reagent was added, and the cells were incubated for 5 min at 37°C in a humidified 5% CO_2 incubator. The cells were transferred into a sterile 15 mL tube and recovered by centrifugation (1,500 rpm, 5 min). After discarding the supernatant, the pellet was resuspended in 1 mL of complete media and transferred to a new T75 flask with 10 mL of complete medium. The cells were then incubated at 37°C in a humidified 5% CO_2 incubator.

2.10.2. Induction of BC tumors

After 1 week of acclimatization, the mice were inoculated with 4T1 murine mammary cancer cells. The 4T1 cells were harvested, resuspended in 1 mL of complete medium, and the cell density was adjusted to 10,000 cells/mL. Then, 100 μL of this cell suspension was inoculated into the left thoracic mammary fat pad of each mouse.³⁸ Tumors became palpable between days 11 and 12 after inoculation.³⁸ Once the tumor was detectable, the mice were randomly assigned to one of four groups (Table 1).

The Vehicle and CO groups received oral gavage of 50 μL soy oil or 2.5 mg of Cur twice daily. The NE and Cur-NE mice received topical application (500 μL) of NE alone (placebo) or Cur-NE over the tumor area twice daily. The treatment continued until the animals were sacrificed 20 days after the tumor was induced.

2.10.3. Measurement of tumor volume

The site of tumor inoculation was palpated every 3 – 4 days. Once the tumor was palpable, a digital caliper was used to measure the tumor size. The tumors' two perpendicular diameters (length, L; width, W) were recorded to calculate

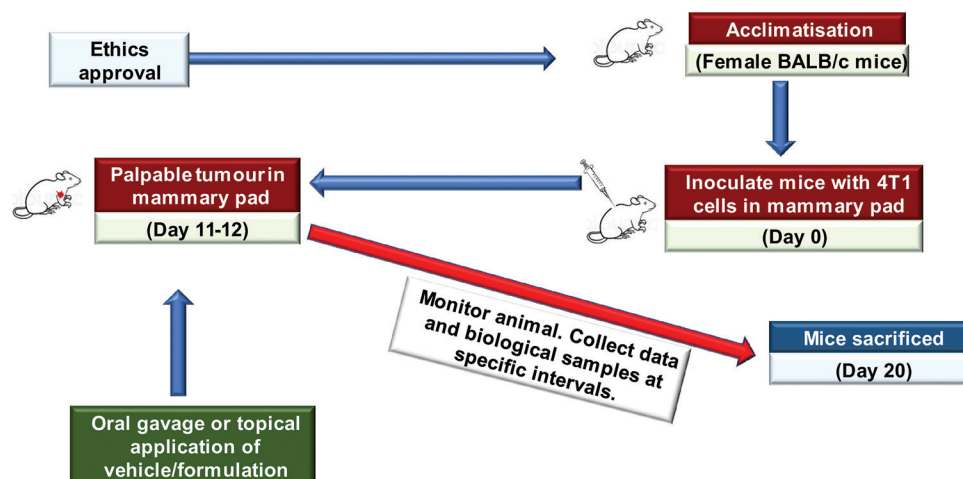


Figure 1. Experimental design for the development of syngeneic breast cancer mouse model

Table 1. Description of different groups of test animals

Group	Description of treatment	Number of animals
Vehicle	Oral gavage with 50 µL of soy oil	6
CO	Oral gavage with 50 µL of Cur (2.5 mg in soy oil)	6
B-NE	Topical application of NE (500 µL) over tumor inoculation site	6
Cur-NE	Topical application of Cur-NE (500 µL) over tumor inoculation site	6

Abbreviations: BC: Breast cancer; B-NE: Blank nanoemulsion; Cur: Curcumin; Cur-NE: Curcumin nanoemulsion; NE: Nanoemulsion.

the tumor volume (V) using the following formula³⁹:

$$V = 0.52 \times L^2 \times W.$$

2.11. Histopathological analysis

The experimental animals were sacrificed at the end of the study. The liver, lungs, and half of the tumor were harvested from each mouse and placed in a 10% phosphate-buffered formalin solution (LabChem Sdn Bhd., Malaysia) for histopathological studies. The second half of the tumors were snap-frozen and stored at -80°C for gene expression analysis.

The formalin-fixed tissues were kept for 1 week before gross sectioning. The samples were then cut into small sections (5 mm), placed into labelled cassettes, and stored in formalin until further tissue processing. Paraffin blocks were prepared, sectioned into 4 µm slices using a microtome, and stained with hematoxylin and eosin (Leica Biosystems, Singapore). Stained sections were mounted with distere-ne-phthalate-xylene and air-dried. The stained slides were analyzed under the light microscope (Nikon eclipse 80i, Japan), for signs of metastasis, necrosis, and apoptosis. The Nottingham grading system (Elston–Ellis modification of the Scarff–Bloom–Richardson grading) was used to evaluate the grade of BC.⁴⁰

2.12. Immunohistochemistry (IHC) analysis

IHC staining was performed according to the manufacturer's instructions. Briefly, 5 µm sections were cut from the tumor blocks and placed on a poly-L-lysine-coated slide (LabChem Sdn. Bhd., Malaysia) for IHC analysis. Three biomarkers were analyzed for IHC: Matrix metalloproteinase-13 (MMP-13; rabbit recombinant monoclonal antibody [mAb]; ab219620; 1:2000 dilution; Abcam Carpinteria, USA),⁴¹ CD9 (rabbit polyclonal antibody; ab223052; 1:100 dilution; Abcam Carpinteria, USA), and tissue inhibitor of metalloproteinases-1 (TIMP-1; rabbit recombinant mAb; ab211926; 1:1000 dilution; Abcam, USA). The intensity and the

percentage of positive cells were assessed for each staining. The intensity of immunostaining in the cytoplasm was scored 0 (no brown particles), 1 (light brown particles), 2 (moderate brown particles), or 3 (dark brown particles). The percentage of stained-positive cells was quantified under a microscope and scored 1 (<25% positive cells), 2 (25 – 50% positive cells), 3 (51 – 75% positive cells), and 4 (>75% positive cells). The staining index (SI) was calculated as the product of the intensity and the percentage of positive staining. The SI values were used to define high (SI ≥ 6) and low (SI <6) expressions of MMP-13. The intensity of CD9 staining was given a score of 0 (negative), 1 (weakly positive), 2 (moderately positive), or 3 (strongly positive). Percentage of positive tumor cells (TC) showing membranous-to-cytoplasmic staining was given a score of 0 (0%), 1 (1 – 25%), 2 (26 – 50%), 3 (51 – 75%), or 4 (>75%). The final CD9 immunoreactivity score (IS; range: 0 – 12) was determined by multiplying the intensity score and the extent score (<https://ejbc.kr/DOIx.php?id=10.4048/jbc.2019.22.e9>).

2.13. Gene expression studies

Total RNA was extracted from tumor tissues stored at -80°C using a commercial RNA extraction kit (Pure NATM Fast spin Total RNA extraction kit, Sigma-Aldrich, Malaysia). RNA concentration was estimated using the Nanoquant™ plate (Tecan Austria GmbH, Austria) and a microplate reader (Tecan Austria GmbH, Austria). All quantifications were performed in triplicates.

For quantitative PCR (qPCR), the RNA samples were thawed and aliquoted to the desired concentration required. The qPCRBIO SyGreen 1-Step kit (PCR Biosystems, USA) was used for cDNA synthesis and PCR by following the manufacturer's protocol. The expression levels of four candidate genes (*CDH-1*, *TWIST 1*, apoptosis inhibitor-5 [*API-5* and *CD-274*], relative to two housekeeping genes (*ACTB*, *GADPH*), were assessed. The reagents used were briefly centrifuged and a master mix was prepared. The threshold cycle (CT) values were obtained using iQ5 software (BioRad, USA) to calculate normalized relative fold expression for the genes of interest. The ΔCT method⁴¹ was used, with the formulas: $\Delta\text{CT} = \text{CT}_{\text{GOI}} - \text{CT}_{\text{HKG}}$ and $\Delta\Delta\text{CT} = \Delta\text{CT} (\text{Treated}) - \Delta\text{CT} (\text{Control})$ where CT_{GOI} is the CT value of the gene of interest, and CT_{HKG} is the average CT of housekeeping genes.

2.14. Statistical analysis

Statistical analysis was carried out using the Statistical Package for the Social Sciences software version 28.0 (IBM, Armonk, USA). Tumor size and tumor weights were collected from the five groups (treatment and control), each containing six mice, and the mean and standard

Table 2. Composition of selected blank nanoemulsion formulations

Code	Oil, Capryol-90 (%)	Smix (%)	Water (%)	Transparent	Homogenous
C-A1	10	40 (30:10 of Tween 20: ethanol)	50	✓	✓
C-A2	15	40 (30:10 of Tween 20: ethanol)	45	✓	✓
C-A3	12.50	40 (30:10 of Tween 20: ethanol)	47.50	✓	✓
C-A4	10	40 (30:10 of Labrafil: Tween 80)	50	Turbid	-
C-A5	12.5	40 (30:10 of Labrafil: Tween 80)	47.50	Turbid	-
C-A6	15	40 (30:10 of Labrafil: Tween 80)	45	Turbid	-
C-A7	10	40 (30:10 of Labrafil: Tween 20)	50	Layer separation	-
C-A8	12.5	40 (30:10 of Labrafil: Tween 20)	47.50	Layer separation	-
C-A9	15	40 (30:10 of Labrafil: Tween 20)	45	Layer separation	-
C-A10	10	40 (Tween 20)	5	✓	✓

Note: Smix: mixture of surfactant and co-surfactant.

deviation (SD) were calculated. A normal distribution was assumed.

Student T-test was performed on the means of the treated groups and the control was compared for the significance with paired T-test. For gene expression studies, an analysis of variance test was used to compare the three treatment groups. The significance level was set at $p < 0.05$ or $p < 0.01$. All data were presented as mean \pm SD.

3. Results and discussion

3.1. Selection of oil and surfactant for NE development

Cur had maximum solubility in Capryol 90 (4.7 ± 0.01 mg/mL), followed by olive oil (2.8 ± 0.01 mg/mL) and corn oil (2.4 ± 0.05 mg/mL). Among the surfactants, maximum solubility was observed with transcutol HP (2.0 ± 0.01 mg/mL), Tween-20 (1.7 ± 0.01 mg/mL), and Tween-80 (0.99 ± 0.01 mg/mL). Tween-20 is a surfactant formed by a polyoxyethylene head group and a single hydrocarbon tail (C12:0). It was selected due to its ability to stabilize NE even at low concentrations. Furthermore, it is non-ionic, less toxic, and biocompatible, which makes it safe to be used in NE formulation.⁴² Thus, Capryol 90 and Tween-20 were selected as the preferred oil and surfactant to develop NE for further evaluation.

3.2. Optimization and characterization of NE

Ten NE-blank formulations (without Cur) were prepared using varying oil, surfactant, and water percentages. Four formulations (C-A1, C-A2, C-A3, and C-A10) were transparent and homogeneous, making them suitable for further characterization, including droplet size, PDI, and ZP. The C-A10 formulation exhibited the smallest droplet size with a suitable PDI, followed by C-A1 (Table 2). Both formulations underwent thermodynamic

Table 3. Analysis of droplet size, polydispersity index (PDI), and zeta-potential (ZP) of selected nanoemulsion formulations

Code	Droplet size (nm)	PDI	ZP (mV)
C-A1	123.53 \pm 2.37	0.323 \pm 0.09	3.48 \pm 0.34
C-A2	252.3 \pm 4.17	0.512 \pm 0.83	4.43 \pm 2.13
C-A3	267 \pm 2.54	0.473 \pm 1.35	0.46 \pm 1.76
C-A10	20.36 \pm 5.2	0.35 \pm 0.34	1.2 \pm 0.35

stability tests. As C-A10 (10% Capryol-90, 40% Tween-20, 50% water) showed better thermodynamic stability, it was used in the development of Cur-NE. The Cur-NE exhibited satisfactory values of droplet size (19.54 ± 0.42 nm), PDI (0.32 ± 0.01), and ZP (-3.98 ± 0.24 mV) (Table 3); it also remained homogeneous after centrifugation, indicating stability under normal storage conditions. It passed all thermodynamic stability tests, with no visible precipitation during prolonged storage, showing good physical stability with no phase separation, creaming, or cracking. The Cur-NE had $62.68 \pm 2.03\%$ drug content of Cur, a pH between 6.02 and 6.79 (within normal skin pH range), and a viscosity of 0.058 ± 0.0013 Pa.s, making it suitable for stable NE and transdermal formulations.

3.3. Storage stability study

The Cur-NE formulation prepared using C-A10 was stored and further analyzed for variation in droplet size, PDI, and drug content over 60 days at 25°C and 4°C. Throughout the study (Day 0, 30, and 60), the droplets remained monodispersed, with size changes of only 1 – 2% (Table 4). The decrease in ZP was not statistically significant, and EE showed no significant variation between 4°C and 25°C, indicating that Cur-NE was relatively stable. The pH (6.02 – 6.79) was within the normal skin range, suggesting

Table 4. Thermodynamic stability of selected nanoemulsion (NE) formulations

Code	Composition (%)			Parameters	Effect of			Overall results
	Oil	Smix	Water		H/C	CENT	F/T	
C-A1	10	40 (30:10 of Tween 20: ethanol)	50	Droplet size (nm)	137.3±7.37	Phase separation	-	Failed
				PDI	0.54±0.73	Phase separation	-	
C-A10	10	40 (Tween-20)	50	Droplet size (nm)	21.37±1.32	Stable, no phase separation	23.36±1.67	Passed
				PDI	0.22±1.78	Stable, no phase separation	0.36±2./02	

Notes: Smix: Mixture of surfactant and co-surfactant; H/C: Heating-cooling cycle; CENT: Centrifugation; F/T: Freeze-thaw cycle; PDI: Polydispersity index; Passed: Acceptable droplet size and PDI values; Failed: Droplet size and PDI value not within an acceptable range, and phase separation was observed.

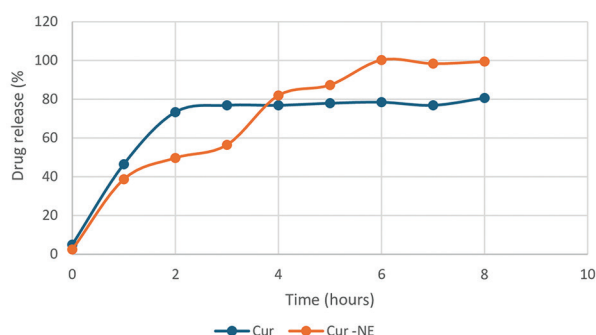


Figure 2. Comparison of the *in vitro* release profile of curcumin-nanoemulsion (Cur-NE) and pure curcumin (Cur) solution at pH 7.4

that Cur-NE would be non-irritating and suitable for transdermal use. Its viscosity (0.058 ± 0.0013 Pa.s) was also appropriate for a stable NE formulation.

3.4. *In vitro* release study using Franz diffusion experiments

At the end of 8 h, Cur-NE formulation showed $99.4 \pm 1.03\%$ release of Cur, which was significantly higher ($p < 0.001$) than the amount of Cur released from a pure Cur solution ($80 \pm 0.13\%$) (Figure 2). The enhanced drug release from Cur-NE can be attributed to the nano-sized droplets, which increase the surface area and facilitate drug release. The significant release profile of Cur-NE, compared to a pure drug solution, suggests its potential for rapid onset of action while also ensuring a prolonged effect of the drug at the administered site.

3.5. Animal model of BC

Rapid tumor growth was observed in the tumor-induced mice that received no treatment (vehicle and CO group) or those that were fed with soy oil (Vehicle group) (Figure 3). However, there was a marked reduction ($p < 0.05$) in the tumor volume in mice that were either fed with Cur (CO group) or treated with topical application of Cur-NE (Cur-NE group) on day 18 (Figure 3).

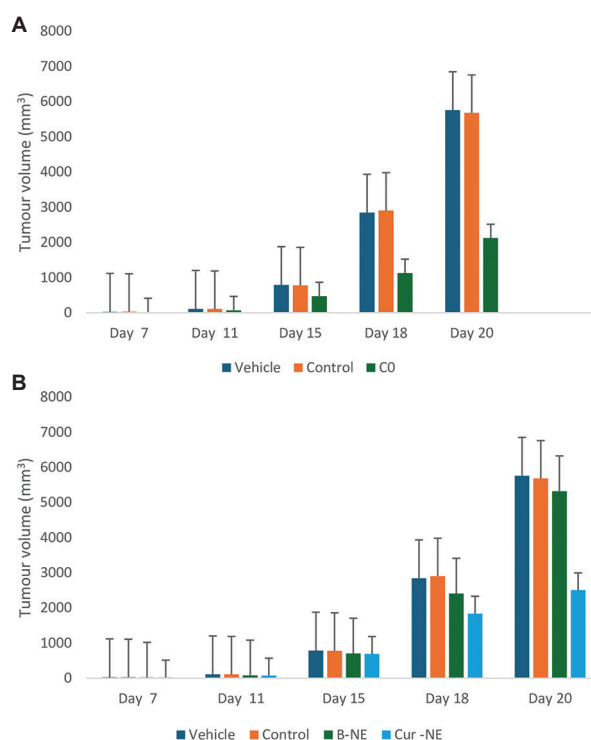


Figure 3. The mean tumor volume. The width and length of the tumor from each animal were recorded once every 4 days from the time the tumor became palpable. The tumor volume from tumor-induced animals that were treated with (A) oral gavage of curcumin (CO) or vehicle and (B) received topical application of blank NE (CNB), curcumin-loaded NE (Cur-NE) is represented as a mean tumor volume \pm standard deviation of six mice ($n=6$) per group at each time-point.

3.6. Histopathological analysis

Histopathological examination was performed on breast tumor, liver, and lung sections from all experimental groups. Tumor sections from Vehicle, CO, and Cur-NE groups showed moderately differentiated infiltrating ductal carcinoma with highly pleomorphic cells. All groups had similar tumor grading using the Nottingham system⁴³ based on tubule formation, nuclear pleomorphism, and mitotic rate. Tumor sections from CO mice showed greater

necrosis (25 – 70%), compared to Vehicle (10 – 50%) or Cur-NE (10 – 40%) mice (Figure 4). Ramalho *et al.*⁴⁴ have suggested that a higher level of tumor necrosis is linked to a potent inhibitory effect on cancer growth. Our study's findings indicate that Cur is a powerful anti-cancer substance that causes necrosis in triple-negative BC (TNBC) tissue. Prior research has demonstrated that the administration of Cur effectively suppressed the growth of tumors and the formation of new blood vessels in a TNBC mouse model.⁴⁵ These findings align with the results of this study, which shows that Cur effectively decreased both the size and weight of the tumor.

3.7. IHC analysis

The 4T1 cell line is a model for TNBC, and it has been the subject of more than 1,000 investigations.⁴⁶ The 4T1 model remains the most clinically relevant pre-clinical animal model for human TNBC.⁴⁷ Non-neoplastic breast epithelial cells were negative for CD9 expression, while necrotic tumor areas showed non-specific staining. Stromal inflammatory cells showed moderate to strong CD9 immunoreactivity, serving as an internal control. Tumors of the Vehicle and CO groups had membranous-to-cytoplasmic CD9 expression in 50 – 75% of TCs with a score of 6. Tumors in the Cur-NE and NEB groups showed the expression in >76% of TCs, scoring 8. Intracellular staining for MMP-13 was localized to the cytoplasm of TCs. Tumors in the Vehicle group showed moderate staining in 51 – 75% of TCs, with a SI of 6. The CO group had moderate staining in >75% of TCs, with a SI of 8, while the CN group showed dark staining in >75% of TCs, with a SI of 12. TIMP-1 expression, mainly in the cytoplasm of TCs, showed moderate intensity in both CO and Cur-NE groups with an SI of 6 in 51 – 75% of TCs (Figure 5).

3.7.1. CD9 expression in BC

CD9 exhibits broad expression in various normal and cancerous tissues.⁴⁸ In a previous study, researchers examined a specific type of BC called invasive carcinoma of no special type. They found that CD9 was highly

expressed in the TCs compared to the normal mammary epithelial cells. The level of CD9 expression varied among the patients. Furthermore, the presence of CD9 in BC tissues was found to be associated with the clinicopathological characteristics of aggressive tumor behavior and poor prognosis. In a study by Baek *et al.*,⁴⁸ CD9 was expressed in 42.5% of invasive lobular carcinoma (ILC) cases, with strong CD9 expression correlating with poor clinical outcomes. The role of CD9 in BC invasion and metastasis likely underpins the observed association between CD9 expression in TCs and unfavorable BC prognosis. CD9 crosslinking triggers intracellular signaling pathways involving molecules such as phosphatidylinositol 4-kinase and Src homology 2, which enhance TC invasiveness by upregulating MMP2 transcription. Furthermore, CD9 interacts with transforming growth factor alpha, inhibiting its cleavage and sustaining epidermal growth factor receptor (EGFR) activation in epithelial cells. This sustained EGFR signaling may promote cellular proliferation, reducing survival rates in CD9-expressing cancer patients. However, no studies have reported CD9 expression in the 4T1 murine model of BC.⁴⁹

3.7.2. MMP-13 expression in BC

Strong fibrillar proteins make up the extracellular matrix (ECM) and epithelial basement membrane. Metastasis and tumor invasion requires the proteolytic enzyme MMP-13 to degrade type II collagen and other ECM proteins, disrupting the structural integrity of tissues and facilitating tumor invasion into surrounding areas.⁵⁰ Recent findings suggest that MMP-13 may be crucial to the extracellular MMP activation cascade that degrades the ECM network.⁵¹ A study found that MMP-13 protein expression was considerably higher in BC cells than in normal breast tissues, suggesting that MMP-13 may be upregulated during human BC growth and progression.⁵² Cur has demonstrated significant potential in downregulating MMP-13 expression, particularly in cancer research.⁵³ In our study, the staining of MMP-13 was higher in the Cur-NE group (SI = 12) than in the CO group (SI = 8), underscoring the efficacy of Cur-NE in downregulating

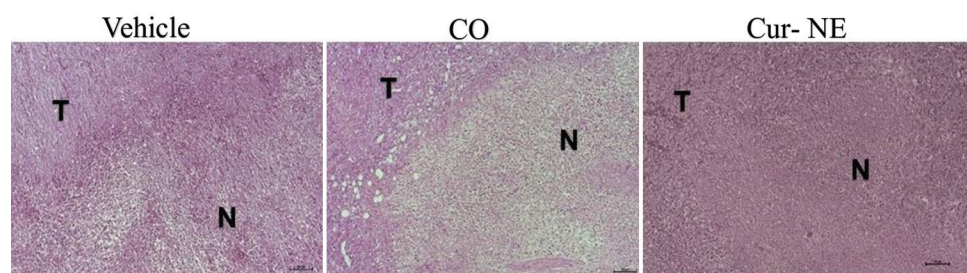


Figure 4. Histopathology analysis of tumor sections from BC mouse models receiving oral soy oil (Vehicle), oral curcumin (CO), or topical application of curcumin-nanoemulsion (Cur-NE). Sections (4 μ m) were stained with haematoxylin and eosin. Magnification: $\times 100$. N indicates necrosis while T indicates moderately differentiated infiltrating duct carcinoma.

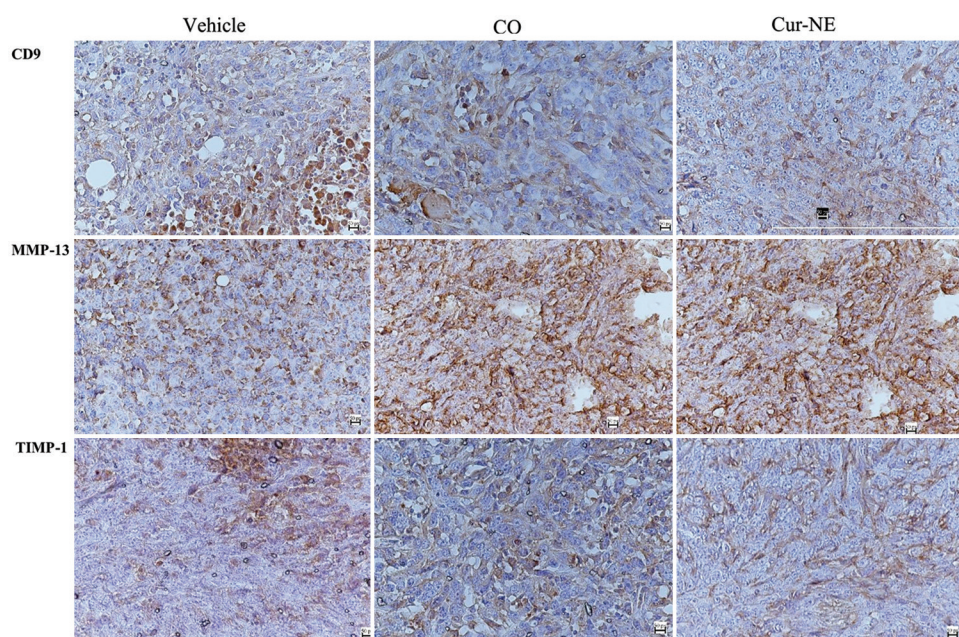


Figure 5. Immunohistochemistry analysis of tumor sections from BC mouse models receiving oral soy oil (Vehicle), oral curcumin (CO), or topical application of curcumin-nanoemulsion. Sections (4 μ m) were stained for CD9, matrix metalloproteinase-13, and tissue inhibitor of metalloproteinases-1. Magnification: $\times 400$.

critical proteins involved in metastasis. This makes Cur, particularly in advanced delivery systems like NE, a promising adjunctive therapy for targeting MMP-13 and its downstream effects on tumor progression.

3.7.3. TIMP-1 expression in BC

TIMP-1 is crucial in BC progression as it modulates MMPs, enzymes that facilitate ECM breakdown and cancer spread.⁵⁴ TIMP-1 suppresses MMPs and prevents excessive matrix degradation; nonetheless, its increased expression in BC correlates with a poor prognosis due to its tumor-promoting roles, such as promoting growth, exerting anti-apoptotic actions, and modulating angiogenesis.⁵⁴ Research indicates elevated TIMP-1 levels in BC tissue relative to benign or normal tissue, with immunodetection predominantly observed in malignant cells and the adjacent stroma.⁵⁵ Research, including a study by Nakopoulou *et al.*,⁵⁵ substantiates that TIMP-1 is markedly overexpressed in breast carcinomas, underscoring its intricate function in tumor biology.

3.8. Gene expression studies

The mean fold changes of selected genes (*TWIST1*, *CDH1*, *API5*, and *CD274*) in the tumors of CO and Cur-NE groups are shown in Figure 6. The results show that Cur exerts its effect on these genes by differentially regulating their expression when compared with the Vehicle group. In tumors from CO, Cur-NE, the expression of the *CDH1*, *API5*, *CD274*, and *TWIST1* genes was downregulated. These

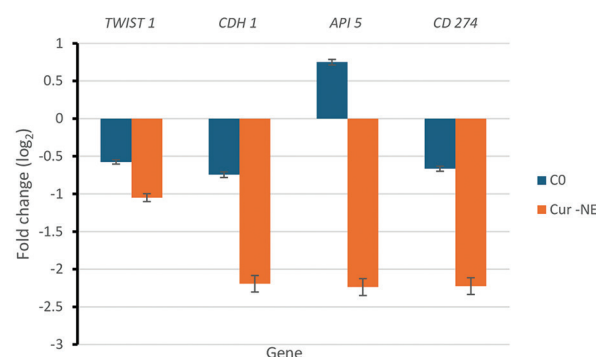


Figure 6. The expression of *TWIST1*, *CDH1*, *API5*, and *CD274* genes in tumors obtained from BC mouse models receiving oral curcumin (CO) or topical application of curcumin-nanoemulsion (Cur-NE). Samples were analyzed using quantitative polymerase chain reaction and data were normalized with a housekeeping gene (*GAPDH*). Results are expressed as log₂ fold change, with expression in tumors from vehicle group as a reference. $n=3$ for each group.

genes are crucial in the development and progression of murine BC. Interestingly, the downregulation of these genes was more significant in tumors from the Cur-NE group compared to the CO group. These findings underscore the effectiveness of topical application of Cur-NE, compared to oral Cur supplementation, in downregulating critical genes involved in TNBC development and progression, highlighting its potential as a targeted therapeutic strategy.

TWIST1, a critical regulator of epithelial-to-mesenchymal transition (EMT), facilitates metastasis by

suppressing epithelial markers such as E-cadherin (CDH1) while promoting mesenchymal traits. The observed reduction in *TWIST1* expression aligns with research demonstrating Cur's ability to inhibit EMT through the *TWIST1*-mediated pathways.⁵⁶ Interestingly, although CDH1 is generally reduced during EMT, its downregulation in our study may reflect a complex regulatory mechanism, possibly influenced by Cur's impact on dynamic cell adhesion processes, as reported in other cancer models.⁵⁷

The *API5* gene, which prevents programmed cell death and supports tumor survival, was notably suppressed following Cur-NE treatment. This finding is consistent with previous studies showing that Cur promotes apoptosis by inhibiting anti-apoptotic regulators.⁵⁸ Moreover, the immune checkpoint gene, *CD274* (encodes for PD-L1 protein), which plays a crucial role in immune evasion, was downregulated. This suggests that Cur-NE may exert immunomodulatory effects, potentially enhancing antitumor immune responses. These results align with prior reports indicating that Cur downregulates PD-L1 expression through the inhibition of NF- κ B pathway.⁵⁹

3.9. Advantages of topical application of Cur-NE

Unlike nanoemulgels, several drug carriers used in topical application – such as liposomes, niosomes, microemulsions, and topical gel – are reported to be confined to the skin surface, leading to poor drug efficacy.²⁹ The nanoemulgels have emerged as an optimal formulation for topical application, offering enhanced and sustained drug release at the targeted site.²⁹ Moreover, this approach improves patients' compliance, avoids first-pass metabolism, reduces side effects, and allows constant drug levels in the blood over extended periods.⁶⁰

4. Future perspectives

Compared to conventional Cur formulations, our results suggest that NE enhances the substance's ability to regulate gene expression patterns, likely due to improved bioavailability and cellular uptake. Given these promising findings, further research should explore whether Cur-NE can be effectively combined with immune checkpoint inhibitors or apoptosis-inducing agents to improve therapeutic outcomes. Future investigations should also focus on elucidating the molecular mechanisms underlying its impact on EMT-related pathways and immune modulation to better define its potential role in TNBC treatment.

Future investigations should also prioritize enhancing the therapeutic relevance of Cur-NE through meticulously structured trials evaluating its efficacy and safety in cancer patients. Clinical studies must investigate appropriate

dosing, bioavailability, and long-term results to ascertain its therapeutic potential. Furthermore, examining Cur-NE alongside established chemotherapeutic drugs, such as paclitaxel or doxorubicin, may augment its anticancer efficacy through synergistic pathways.^{24,28} Subsequent pre-clinical investigations must evaluate toxicity and pharmacokinetics to ensure a thorough comprehension of its systemic distribution, metabolism, and possible adverse consequences.²³ This research can potentially enable the transition of Cur-NE as an effective anticancer treatment from bench to bedside.

5. Conclusion

This study demonstrates the therapeutic potential of Cur-NE as an effective delivery system for targeting key molecular pathways involved in TNBC progression. The optimized Cur-NE formulation exhibited enhanced stability and superior release of Cur compared to free Cur. The oral Cur and topical Cur-NE treatments downregulated the expression of critical genes (*CDH1*, *API5*, *CD274*, and *TWIST1*) associated with tumor development and progression, with the topical application showing significantly greater efficacy. Furthermore, the IHC analysis revealed reduced expression of metastatic markers (MMP-13, TIMP-1, and CD9) in breast tumor tissues from mice models treated with Cur-NE. These findings suggest that Cur-NE holds promise as a targeted therapeutic strategy, offering significant advantages over conventional Cur supplementation. Future studies are warranted to further explore its clinical applicability and mechanism of action.

Acknowledgements

The authors would like to thank the IMU University (formerly known as International Medical University) for providing the research grant that supported this study.

Funding

This study was supported by a research grant from the (IMU 357/2016).

Conflict of interest

The authors declare no conflict of interest.

Author contributions

Conceptualization: Htar Htar Aung, Ammu Kutty Radhakrishnan, Shadab Md

Investigation: Anupa Sivakumar, Sunil Pazhayanur Venkateswaran, Jeya Seela Anandha Rao, Shadab Md

Methodology: Sunil Pazhayanur Venkateswaran, Jeya Seela Anandha Rao, Ammu Kutty Radhakrishnan, Shadab Md

Writing-original draft: Anupa Sivakumar, Sunil Pazhayannur Venkateswaran, Ammu Kutty Radhakrishnan

Writing-review & editing: Anupa Sivakumar, Sunil Pazhayannur Venkateswaran, Ammu Kutty Radhakrishnan

Ethics approval and consent to participate

This study was approved by the joint research and ethics committee of the (IMU 357/2016).

Consent for publication

Not applicable.

Availability of data

Data are available from the corresponding author upon reasonable request.

References

1. Sung H, Ferlay J, Siegel RL, *et al.* Global cancer statistics 2020: GLOBOCAN estimates of incidence and mortality worldwide for 36 cancers in 185 countries. *CA Cancer J Clin.* 2021;71(3):209-249.
doi: 10.3322/caac.21660
2. Ferlay J, Colombet M, Soerjomataram I, *et al.* Cancer statistics for the year 2020: An overview. *Int J Cancer.* 2021;71:209-249.
doi: 10.1002/ijc.33588
3. Termizi NA. *Cancer Registry Report*. Available from: <https://nci.moh.gov.my/index.php/ms/pengumuman/797-cancer-registry-report> [Last accessed on 2024 Nov 24].
4. World Cancer Research Fund. *Breast Cancer Statistics*. Available from: <https://www.wcrf.org/cancer-trends/breast-cancer-statistics> [Last accessed on 2024 Nov 24].
5. *Breast Cancer Treatment (PDQ®): Patient Version. PDQ Cancer Information Summaries*; 2002.
6. Weber WP, Soysal SD, Kappos EA, Babst D, Haug M. Current standards in oncoplastic breast conserving surgery. *Breast.* 2017;32:S14.
doi: 10.1016/s0960-9776(17)30084-x
7. Orecchia R. Radiation therapy for inflammatory breast cancer. *Eur J Surg Oncol.* 2018;44(8):1148-1150.
doi: 10.1016/j.ejso.2018.05.015
8. Abotaleb M, Kubatka P, Caprnda M, *et al.* Chemotherapeutic agents for the treatment of metastatic breast cancer: An update. *Biomed Pharmacother.* 2018;101:458-477.
doi: 10.1016/j.biopha.2018.02.108
9. Ju J, Zhu AJ, Yuan P. Progress in targeted therapy for breast cancer. *Chronic Dis Transl Med.* 2018;4(3):164-175.
doi: 10.1016/j.cdtm.2018.04.002
10. Patani N, Mokbel K. Herceptin and breast cancer: an overview for surgeons. *Surg Oncol.* 2010;19(1):e11-21.
doi: 10.1016/j.suronc.2008.11.001
11. Verstappen CC, Heimans JJ, Hoekman K, Postma TJ. Neurotoxic complications of chemotherapy in patients with cancer: Clinical signs and optimal management. *Drugs.* 2003;63(15):1549-1563.
doi: 10.2165/00003495-200363150-00003
12. van Dam FS, Schagen SB, Muller MJ, *et al.* Impairment of cognitive function in women receiving adjuvant treatment for high-risk breast cancer: High-dose versus standard-dose chemotherapy. *J Natl Cancer Inst.* 1998;90(3):210-218.
doi: 10.1093/jnci/90.3.210
13. Jordan K, Kasper C, Schmoll HJ. Chemotherapy-induced nausea and vomiting: Current and new standards in the antiemetic prophylaxis and treatment. *Eur J Cancer.* 2005;41(2):199-205.
doi: 10.1016/j.ejca.2004.09.026
14. McQuade RM, Bornstein JC, Nurgali K. Anti-colorectal cancer chemotherapy-induced diarrhoea: Current treatments and side-effects. *Int J Clin Med.* 2014;5(7):393-406.
doi: 10.4236/ijcm.2014.57054
15. Gottardis MM, Robinson SP, Satyaswaroop PG, Jordan VC. Contrasting actions of tamoxifen on endometrial and breast tumor growth in the athymic mouse. *Cancer Res.* 1988;48(4):812-815.
16. Levine MN. Prevention of thrombotic disorders in cancer patients undergoing chemotherapy. *Thromb Haemost.* 1997;78(1):133-136.
doi: 10.1055/s-0038-1657515
17. Jordan VC. Tamoxifen: Toxicities and drug resistance during the treatment and prevention of breast cancer. *Annu Rev Pharmacol Toxicol.* 1995;35(1):195-211.
doi: 10.1146/annurev.pharmtox.35.1.195
18. Pratheeshkumar P, Sreekala C, Zhang Z, *et al.* Cancer prevention with promising natural products: mechanisms of action and molecular targets. *Anticancer Agents Med Chem.* 2012;12(10):1159-1184.
doi: 10.2174/187152012803833035
19. Menon VP, Sudheer AR. Antioxidant and anti-inflammatory properties of curcumin. In: *Advances in Experimental Medicine and Biology*. United States: Springer; 2007. p. 105-125.
20. Nelson KM, Dahlin JL, Bisson J, Graham J, Pauli GF, Walters MA. The essential medicinal chemistry of curcumin: Miniperspective. *J Med Chem.* 2017;60(5):1620-1637.
doi: 10.1021/acs.jmedchem.6b00975
21. Anand P, Thomas SG, Kunnumakkara AB, *et al.* Biological

- activities of curcumin and its analogues (Congeners) made by man and mother nature. *Biochem Pharmacol*. 2008;76(11):1590-1611.
doi: 10.1016/j.bcp.2008.08.008
22. Bansal SS, Goel M, Aqil F, Vadhanam MV, Gupta RC. Advanced drug delivery systems of curcumin for cancer chemoprevention. *Cancer Prev Res (Phila)*. 2011;4(8):1158-1171.
doi: 10.1158/1940-6207.CAPR-10-0006
23. Yallapu MM, Jaggi M, Chauhan SC. Curcumin nanoformulations: A future nanomedicine for cancer. *Drug Discov Today*. 2012;17(1-2):71-80.
doi: 10.1016/j.drudis.2011.09.009
24. Anand P, Kunnumakkara AB, Newman RA, Aggarwal BB. Bioavailability of curcumin: Problems and promises. *Mol Pharm*. 2007;4:807-18.
25. Preeti, Sambhakar S, Malik R, *et al*. Nanoemulsion: An emerging novel technology for improving the bioavailability of drugs. *Scientifica (Cairo)*. 2023;2023:6640103.
doi: 10.1155/2023/6640103
26. Sharma S, Pawar S, Jain UK. Development and evaluation of topical gel of curcumin from different combination of polymers formulation and evaluation of herbal gel. *Int J Pharm Pharm Sci*. 2012;4(4):452-456.
27. Siegel RL, Miller KD, Fuchs HE, Jemal A. Cancer statistics, 2023. *CA Cancer J Clin*. 2023;73(1):17-48.
doi: 10.3322/caac.21763
28. Prasad S, Gupta SC, Aggarwal BB. Serendipity in cancer drug discovery: Revisiting the anticancer properties of curcumin. *Trends Pharmacol Sci*. 2016;37(10):889-905.
29. Pulaski BA, Terman DS, Khan S, Muller E, Ostrand-Rosenberg S. Cooperativity of Staphylococcal aureus enterotoxin B superantigen, major histocompatibility complex class II, and CD80 for immunotherapy of advanced spontaneous metastases in a clinically relevant postoperative mouse breast cancer model. *Cancer Res*. 2000;60(10):2710-2715.
30. Ma P, Zeng Q, Tai K, *et al*. Preparation of curcumin-loaded emulsion using high pressure homogenization: Impact of oil phase and concentration on physicochemical stability. *Lebenson Wiss Technol*. 2017;84:34-46.
doi: 10.1016/j.lwt.2017.04.074
31. Ahmad N, Ahmad R, Al-Qudaihi A, *et al*. Preparation of a novel curcumin nanoemulsion by ultrasonication and its comparative effects in wound healing and the treatment of inflammation. *RSC Adv*. 2019;9(35):20192-20206.
doi: 10.1039/c9ra03102b
32. Marwa A, Iskandarsyah, Jufri M. Nanoemulsion curcumin injection showed significant anti-inflammatory activities on carrageenan-induced paw edema in Sprague-Dawley rats. *Heliyon*. 2023;9(4):e15457.
doi: 10.1016/j.heliyon.2023.e15457
33. Lee J, Sah H. Preparation of PLGA nanoparticles by milling spongelike PLGA microspheres. *Pharmaceutics*. 2022;14(8):1540.
doi: 10.3390/pharmaceutics14081540
34. Kaur L, Singh K, Paul S, Singh S, Singh S, Jain SK. A Mechanistic study to determine the structural similarities between artificial membrane strat-MTM and biological membranes and its application to carry out skin permeation study of amphotericin B nanoformulations. *AAPS PharmSciTech*. 2018;19(4):1606-1624.
doi: 10.1208/s12249-018-0959-6
35. Radhakrishnan AK, Sim GC, Cheong SK. Comparing the ability of freshly generated and cryopreserved dendritic cell vaccines to inhibit growth of breast cancer in a mouse model. *Biores Open Access*. 2012;1(5):239-246.
doi: 10.1089/biores.2012.0229
36. Pulaski BA, Ostrand-Rosenberg S. Mouse 4T1 breast tumor model. In: *Current Protocols in Immunology*. Ch. 20. United States: Wiley; 2001.
doi: 10.1002/0471142735.im2002s39
37. Rajaratnam H, Rasudin NS, Safuan S, Abdullah NA, Mokhtar NF, Mohd Fuad WE. Passage Number of 4T1 cells influences the development of tumour and the progression of metastasis in 4T1 orthotopic mice. *Malays J Med Sci*. 2022;29(3):30-42.
doi: 10.21315/mjms2022.29.3.4
38. Subramaniam S, Anandha Rao JS, Ramdas P, *et al*. Reduced infiltration of regulatory T cells in tumours from mice fed daily with gamma-tocotrienol supplementation. *Clin Exp Immunol*. 2021;206(2):161-172.
doi: 10.1111/cei.13650
39. Tomayko MM, Reynolds CP. Determination of subcutaneous tumor size in athymic (nude) mice. *Cancer Chemother Pharmacol*. 1989;24(3):148-154.
doi: 10.1007/bf00300234
40. Edge SB, Compton CC. The American Joint Committee on Cancer: The 7th edition of the AJCC cancer staging manual and the future of TNM. *Ann Surg Oncol*. 2010;17(6):1471-1474.
doi: 10.1245/s10434-010-0985-4
41. Rao X, Huang X, Zhou Z, Lin X. An improvement of the 2⁻(-delta delta CT) method for quantitative real-time polymerase chain reaction data analysis. *Biostat Bioinform Biomath*. 2013;3(3):71-85.
42. Kim J, Kwak S, Park MS, *et al*. Safety verification for

- polysorbate 20, pharmaceutical excipient for intramuscular administration, in Sprague-Dawley rats and New Zealand White rabbits. *PLoS One*. 2021;16(8):e0256869.
doi: 10.1371/journal.pone.0256869
43. Rachmawati H, Budiputra DK, Mauludin R. Curcumin nanoemulsion for transdermal application: formulation and evaluation. *Drug Dev Ind Pharm*. 2015;41(4):560-566.
doi: 10.3109/03639045.2014.884127
 44. Ramalho RT, Aydos RD, Schettert I, Cassino PC. Histopathological evaluation of tumor necrosis and volume after cyanogenic chemotherapy. *Acta Cir Bras*. 2014;29 Suppl 2:38-42.
doi: 10.1590/s0102-8650201400140008
 45. Farghadani R, Naidu R. Curcumin as an enhancer of therapeutic efficiency of chemotherapy drugs in breast cancer. *Int J Mol Sci*. 2022;23(4):2144.
doi: 10.3390/ijms23042144
 46. Arroyo-Crespo JJ, Armiñán A, Charbonnier D, *et al*. Characterization of triple-negative breast cancer preclinical models provides functional evidence of metastatic progression. *Int J Cancer*. 2019;145(8):2267-2281.
doi: 10.1002/ijc.32270
 47. Li Q, Li M, Zheng K, Tang S, Ma S. Expression pattern analysis and drug differential sensitivity of cancer-associated fibroblasts in triple-negative breast cancer. *Transl Oncol*. 2021;14(1):100891.
doi: 10.1016/j.tranon.2020.100891
 48. Baek J, Jang N, Choi JE, Kim JR, Bae YK. CD9 expressions in tumor cells is associated with poor prognosis in patients with invasive lobular carcinoma. *J Breast Cancer*. 2019;22(1):77-85.
doi: 10.4048/jbc.2019.22.e9
 49. Visse R, Nagase H. Matrix metalloproteinases and tissue inhibitors of metalloproteinases: structure, function, and biochemistry: Structure, function, and biochemistry. *Circ Res*. 2003;92(8):827-839.
doi: 10.1161/01.RES.0000070112.80711.3D
 50. Umamaheswari A, Katari S, Pasala C, *et al*. Pathophysiology of matrix metalloproteinases in breast cancer progression. *J Clin Sci Res*. 2019;8(3):145.
doi: 10.4103/jcsr.jcsr_67_19
 51. Zhang B, Cao X, Liu Y, *et al*. Tumor-derived matrix metalloproteinase-13 (MMP-13) correlates with poor prognoses of invasive breast cancer. *BMC Cancer*. 2008;8(1):83.
doi: 10.1186/1471-2407-8-83
 52. Kudo Y, Iizuka S, Yoshida M, *et al*. Matrix metalloproteinase-13 (MMP-13) directly and indirectly promotes tumor angiogenesis. *J Biol Chem*. 2012;287(46):38716-38728.
doi: 10.1074/jbc.M112.373159
 53. Wang J, Ma J, Gu JH, *et al*. Regulation of type II collagen, matrix metalloproteinase-13 and cell proliferation by interleukin-1 β is mediated by curcumin via inhibition of NF- κ B signaling in rat chondrocytes. *Mol Med Rep*. 2017;16(2):1837-1845.
doi: 10.3892/mmr.2017.6771
 54. Wurtz SØ, Schrohl AS, Sørensen NM, *et al*. Tissue inhibitor of metalloproteinases-1 in breast cancer. *Endocr Relat Cancer*. 2005;12(2):215-227.
doi: 10.1677/erc.1.00719
 55. Nakopoulou L, Giannopoulou I, Stefanaki K, *et al*. Enhanced mRNA expression of tissue inhibitor of metalloproteinase-1 (TIMP-1) in breast carcinomas is correlated with adverse prognosis. *J Pathol*. 2002;197(3):307-313.
doi: 10.1002/path.1129
 56. Puisieux A, Brabletz T, Caramel J. Oncogenic roles of EMT-inducing transcription factors. *Natl Cell Biol*. 2014;16(6):488-494.
doi: 10.1038/ncb2976
 57. Roy S, Majumdar AP. Curcumin inhibits *twist1* and restores E-cadherin expression by upregulating miR-200 in colon cancer cells. *Cancer Lett*. 2012;325(1):41-51.
 58. Jin H, Qiao F, Wang Y, Xu Y, Shang Y. Curcumin inhibits cell proliferation and induces apoptosis of human non-small cell lung cancer cells through the upregulation of miR-192-5p and suppression of PI3K/Akt signaling pathway. *Oncol Rep*. 2015;34(5):2782-2789.
doi: 10.3892/or.2015.4258
 59. Shakeri A, Sahebkar A, Javadi B, *et al*. Curcumin suppresses the expression of PD-L1 in breast cancer cells via inhibition of NF- κ B signaling. *Pharmacol Res*. 2019;147:104353.
 60. Rani D, Singh C, Kumar A, Sharma VK. Formulation development and *in-vitro* evaluation of minoxidil bearing glycosomes. *Am J Biomed Res*. 2016;4:27-37.
doi: 10.12691/ajbr-4-2-1